Determination of Structural Features of Electrogenerated *trans*-[MoCl(NMe)($Ph_2PCH_2CH_2PPh_2)_2]^{2+}$ by Multinuclear Electron Paramagnetic Resonance and Electron Nuclear Double Resonance Spectroscopy and Comparison of Interatomic Distances with those measured by *X*-Ray Analysis of the Parent Monocation†

David L. Hughes, David J. Lowe,* Modher Y. Mohammed, Christopher J. Pickett,* and Nelson M. Pinhal
AFRC Institute of Plant Science Research, Nitrogen Fixation Laboratory, University of Sussex, Brighton BN1 9RQ

The 17-electron dication *trans*-[MoCl(NMe)($Ph_2PCH_2CH_2PPh_2)_2]^{2+}$ was electrogenerated as a stable solution species in a trifluoroacetic acid electrolyte and its structure deduced by analysis of multinuclear e.p.r. and electron nuclear double resonance spectra. Certain interatomic distances within this molybdenum(IV) dication were calculated from the magnitude of anisotropic dipolar interactions obtained from field-dependent ENDOR frequency-shift measurements and comparisons made with distances measured by *X*-ray analysis of the parent monocation. It is concluded that the {MoNMe} group in the 17-electron product retains the geometric configuration of its 18-electron precursor.

The methylimide ligand (NMe) in *trans*-[MoCl(NMe)($Ph_2PCH_2CH_2PPh_2)_2]^+$ (**1**) can be transformed to ligating cyanide by removal of protons and electrons or to free methylamine by their addition, Scheme 1.[1,2] These reactions may bear upon both biological reduction of cyanide by nitrogenase[3,4] and the diversification of nitrogen-containing products that can be synthesised *via* reactions of ligating dinitrogen.[5]

In this paper we report the nature of the primary oxidation of complex (**1**), the stabilisation of the initial product of electron transfer, (**2**), and the characterisation of this product by e.p.r. and multinuclear electron nuclear double resonance (ENDOR) spectroscopy.

Although somewhat akin to multinuclear n.m.r. spectroscopy of diamagnetics, the application of ENDOR techniques to paramagnetic co-ordination complexes is not extensive. Here we show the value of ENDOR spectroscopy on frozen solutions in the identification of atoms and groups within a paramagnetic compound that has been generated by *ex situ* anodic oxidation.

The observation of fast, reversible electron-transfer chemistry usually signals minimal inner-sphere structural reorganisation but this is not rigidly diagnostic.[6] We wished to determine whether the removal of an electron from complex (**1**) results in rearrangement of the {MoNMe} group for example as illustrated by the rehybridisation in Scheme 2.

We have therefore analysed anisotropic dipolar interactions, obtained from field-dependent ENDOR frequency-shift measurements, and these have allowed the calculation of certain interatomic distances within the {MoNMe} group of the product (**2**) and in its ^{13}C methyl-labelled counterpart. These distances are compared with those which we have determined for the parent (**1**) by an *X*-ray crystal structure analysis, as described in detail below.

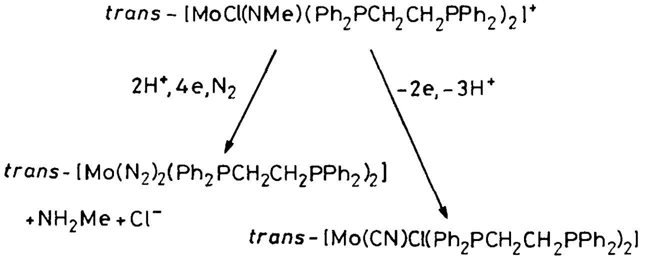

Scheme 1.

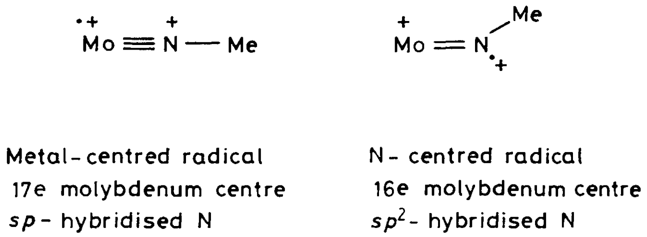

Scheme 2. Possible hybridisations of the methylimide ligand

Results and Discussion

The Parent Complex (**1**): *Description of the Molecular and Crystal Structure of trans*-[MoCl(NMe)($Ph_2PCH_2CH_2PPh_2)_2$]PF_6·CH_2Cl_2.—The complex cations have a distorted octahedral co-ordination arrangement, with the chloro-group *trans* to the methylimide ligand. Figure 1 shows the molecular structure with appropriate labelling of the atoms. The four P atoms form a very shallow tetrahedron about the 'equatorial plane,' each P atom being *ca.* 0.05 Å from the mean plane, and the Mo atom is displaced 0.16 Å from this plane towards the methylimido-group. The dimensions about the metal atom (Table 1) are very similar to those in the closely related molybdenum(IV) cation *trans*-[MoBr(NH)($Ph_2PCH_2CH_2PPh_2)_2]^+$ (ref. 7) and in the tungsten(IV) complex [WCl_2(NPh)($PMe_3)_3$].[8] The Mo–N–C group is essentially linear, with bond lengths that confirm a multiple Mo–N bond and a single N_{sp}–C_{sp^3} bond. Each of the methyl H atoms, refined under geometrical restraints, has close contacts with the phenyl groups which fold around the methylimide group. In the refined

---

† *Supplementary data available:* see Instructions for Authors, *J. Chem. Soc., Dalton Trans.*, 1990, Issue 1, pp. xix–xxii.

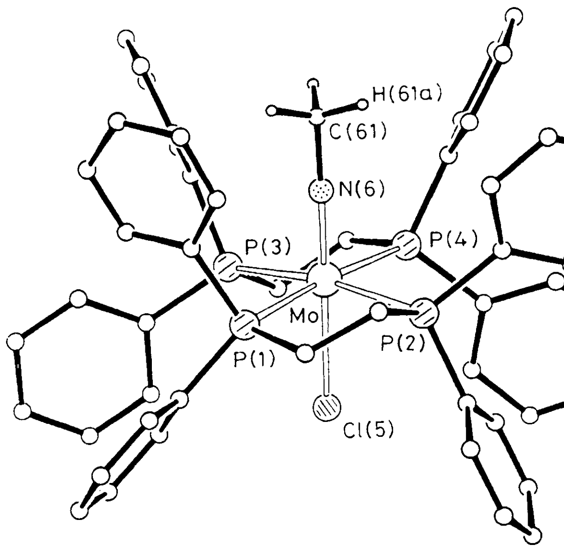

Figure 1. A view of the structure of the parent cation, *trans*-$[MoCl(NMe)(Ph_2PCH_2CH_2PPh_2)_2]^+$, (**1**)

Table 1. Selected molecular dimensions (lengths in Å, angles in °) in $[MoCl(NMe)(Ph_2PCH_2CH_2PPh_2)_2]PF_6{\cdot}CH_2Cl_2$ with estimated standard deviations (e.s.d.s) in parentheses

(*a*) About the Mo atom

Mo–P(1)	2.547(2)	Mo–P(4)	2.551(2)
Mo–P(2)	2.532(2)	Mo–Cl(5)	2.492(2)
Mo–P(3)	2.558(2)	Mo–N(6)	1.733(5)
P(1)–Mo–P(2)	79.5(1)	P(2)–Mo–N(6)	91.4(2)
P(1)–Mo–P(3)	101.3(1)	P(3)–Mo–P(4)	78.9(1)
P(1)–Mo–P(4)	175.0(1)	P(3)–Mo–Cl(5)	81.6(1)
P(1)–Mo–Cl(5)	87.7(1)	P(3)–Mo–N(6)	98.1(2)
P(1)–Mo–N(6)	91.3(2)	P(4)–Mo–Cl(5)	87.5(1)
P(2)–Mo–P(3)	170.4(1)	P(4)–Mo–N(6)	93.5(2)
P(2)–Mo–P(4)	99.5(1)	Cl(5)–Mo–N(6)	178.9(2)
P(2)–Mo–Cl(5)	88.9(1)		

(*b*) Torsion angles in the diphosphine ligands

P(1)–C(1)–C(2)–P(2)	−50.7(6)	P(3)–C(3)–C(4)–P(4)	52.8(6)

(*c*) In the methylimide ligand

N(6)–C(61)	1.429(9)	Mo–N(6)–C(61)	177.7(5)

positions, the Mo ... H distances are 3.64, 3.62, and 3.61 Å and the Mo ... C distance is 3.161(8) Å.

The hydrogen atoms of the solvent, CH_2Cl_2, each interact with neighbouring ions: the C(9)–H(9a) ··· Cl(5) interaction with the cation may be considered a 'weak hydrogen bond,' with H ··· Cl 2.66 Å and C–H ··· Cl 141°, and H(9b) is directed towards F(72) of an anion, distance 2.57Å. Other intermolecular contacts are at normal van der Waals distances.

Electrochemical Oxidation of Complex (**1**): *Stabilisation of the One-electron Oxidation Product in a Trifluoroacetic Acid Electrolyte.*—Cyclic voltammetry in dichloromethane or methyl cyanide containing 0.2 mol dm^{-3} $[NBu_4][BF_4]$ at platinum or vitreous carbon electrodes shows that *trans*-$[MoCl(NMe)(Ph_2PCH_2CH_2PPh_2)_2]^+$ (**1**) undergoes a diffusion-controlled, reversible one-electron oxidation consistent with reaction (1).

$$trans\text{-}[MoCl(NMe)(Ph_2PCH_2CH_2PPh_2)_2]^+ \underset{+e}{\overset{-e}{\rightleftharpoons}} trans\text{-}[MoCl(NMe)(Ph_2PCH_2CH_2PPh_2)_2]^{2+} \quad (1)$$

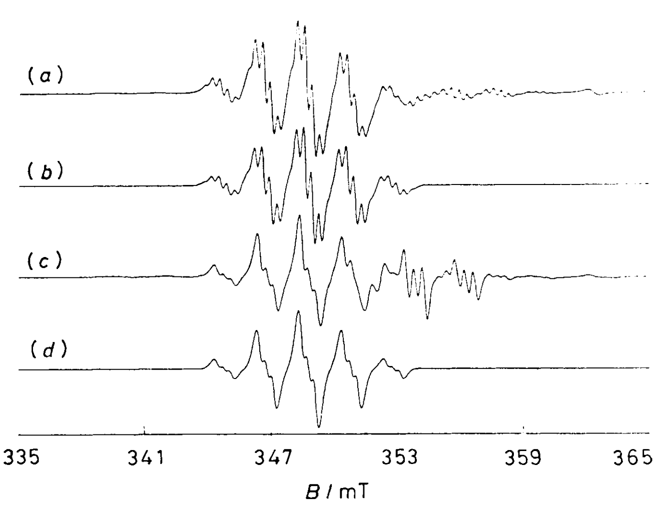

Figure 2. (*a*) Liquid solution e.p.r. spectrum at 290 K of complex (**2**) with the natural-abundance isotope mixture at microwave frequency 9.78 GHz and power 20 mW using 0.1-mT field modulation at 100 kHz. (*c*) Spectrum of (**2**) with ^2H substitution of the methyl protons. (*b*) and (*d*), Simulations of (*a*) and (*c*) respectively using the parameters given in Table 2

However, attempts to synthesise the product (**2**) by bulk electrolyses in either solvent were unsuccessful: multi-electron oxidations were observed because (**2**) was unstable in these media on the time-scale of preparative electrolysis. Trifluoroacetic acid has been shown to be a useful electrochemical solvent of low nucleophilicity in which certain organic[9] and organometallic[10] radical cations have been stabilised. We therefore used an electrolyte based on this solvent in an attempt to prepare (**2**).

Controlled-potential electrolysis of complex (**1**) in trifluoroacetic acid containing 10% trifluoroacetic anhydride and 0.2 mol dm^{-3} $[NBu_4][BF_4]$ at +0.5 V *versus* the ferrocenium–ferrocene couple at a platinum anode gave a dark red-brown solution containing the primary product. Thus the cell current decayed linearly with charge passed in an overall 1 F mol^{-1} process and comparison of the cyclic voltammetry of the anolyte before and after electrolysis showed that (**2**) was formed in >90% yield. Reversal coulometry at +0.1 V regenerated the pink solution of the starting material (**1**) and voltammetry confirmed the essential reversibility of the system.

We attempted to isolate crystals of complex (**2**) in order to determine its structure but this was unsuccessful, as were attempts to isolate the dication from solutions prepared by oxidation of (**1**) with $[NO][PF_6]$. We therefore turned to e.p.r. and ENDOR spectroscopy on the anolyte solution to obtain structural information.

Structural Information from Solution and Frozen-solution E.P.R. Spectra.—The room-temperature e.p.r. spectrum of the anolyte containing complex (**2**) is shown in Figure 2(*a*). This figure also shows a spectrum obtained from electro-oxidation of the $[^2H]$methyl analogue of (**1**), Figure 2(*c*), together with simulations [2(*b*) and (*d*)] obtained using the parameters given in Table 2. The spectrum is that of a single major species (*ca.* 95%) with a minor component (*ca.* 5%) at high field. The major species exhibits coupling to four equivalent ^{31}P atoms, three equivalent $^1H(^2H)$ atoms, and one ^{14}N atom.

Thus we observe large hyperfine coupling to four equivalent ^{31}P atoms indicative of significant delocalisation of spin density onto phosphorus and of the retention of the essentially square-planar array of these atoms about the central Mo atom.

Table 2. Parameters used for simulations of the liquid solution e.p.r. spectra shown in Figure 2(*b*) and (*d*)

g_{iso}	2.004
A_{iso} (^{31}P)	56.1 MHz
A_{iso} (^{14}N)	9.5 MHz
A_{iso} (^{1}H)	10.1 MHz
Half linewidth	3.6 MHz

Table 3. Parameters used for simulations of the frozen-solution e.p.r. spectrum shown in Figure 3(*b*); g and $A(^{31}P)$ were assumed to have parallel principal axes

g_{xx}	2.028
g_{yy}	1.997
g_{zz}	1.988
A_{xx} (^{31}P)	67.5 MHz
A_{yy} (^{31}P)	32.5 MHz
A_{zz} (^{31}P)	65.0 MHz
Half linewidth	19 MHz

Table 4. Hyperfine, distance, and spin-density values determined from e.p.r. and ENDOR spectra of complex (**2**); A_{iso} and A_{dip} were measured for each nucleus as described in the text. The distance r(Å) from the centre of unpaired electron spin density (at the Mo) to each nucleus was determined from A_{dip} assuming a point-dipole interaction. The *s*-orbital spin density was calculated from A_{iso} as described by Morton and Preston.[12] n.d. = Not determined

Nucleus	A_{iso}/MHz	A_{dip}/MHz	r/Å	*s*-Orbital spin density (%)
Each methyl ^{1}H	10.5	4.2	3.8	0.7
Methyl ^{13}C	3.5	1.5	3.2	0.1
^{14}N	10	n.d.	n.d.	0.6
$^{35,37}Cl$	*ca.* 1	n.d.	n.d.	0.02
Each ^{31}P	62	n.d.	n.d.	0.5

The assignment of the three equivalent ^{1}H atoms observed in the room-temperature e.p.r. spectrum of complex (**2**), Figure 2(*a*), to the methyl hydrogens is straightforward. Electro-oxidation of [^{2}H]methyl-labelled (**1**) gives the e.p.r. spectrum in Figure 2(*c*) in which the hyperfine interactions associated with the methyl ^{1}H atoms have disappeared. This is because although ^{2}H has $I = 1$, its magnetic moment is much less than that of ^{1}H and therefore the resultant splitting into three lines cannot be observed.

Hyperfine structure associated with retention of the single nitrogen atom is evident and included in the simulation. Unequivocal confirmation of the assignment of the N-hyperfine structure comes from ENDOR experiments on (**2**) as described below.

Figure 3(*a*) shows the frozen-solution e.p.r. spectrum of the anolyte at 20 K together with a simulation [Figure 3(*b*)] using the parameters listed in Table 3. These parameters, when averaged, are concordant with the values of the isotropic g and ^{31}P-hyperfine couplings of the room-temperature spectra (Table 2). In the amplified frozen-solution spectrum, $^{95,97}Mo$ hyperfine couplings are evident, Figure 3(*a*). We are unable to determine with which g value the hyperfine lines are associated, although we can say that there must be at least one component with $A \geqslant 50 \times 10^{-4}$ cm^{-1} from the extreme low-field components of the $I = 0$ and $-\frac{5}{2}$ transitions (Figure 3); this is a normal value for Mo^{V} in which unpaired spin density resides principally on the Mo atom.[11]

We were unable to observe $^{35,37}Cl$ hyperfine interactions in the solution e.p.r. spectra of the anolyte. Also perturbations of the e.p.r. spectrum were not observed for samples prepared by electro-oxidation of a [^{13}C]methyl-labelled complex. However ENDOR spectroscopy has allowed us to obtain information on both of these nuclei, including *s*-orbital spin-density estimates. This complements spin-density data determined for nitrogen, phosphorus, and hydrogen (methyl) atoms by e.p.r. spectroscopy, Table 4,[12] but perhaps the most important contribution from the ENDOR spectroscopy is that it has allowed interatomic distances to be estimated from measurements on a frozen anolyte and these have enabled us to deduce the arrangement of the methylimidomolybdenum group in the primary product.

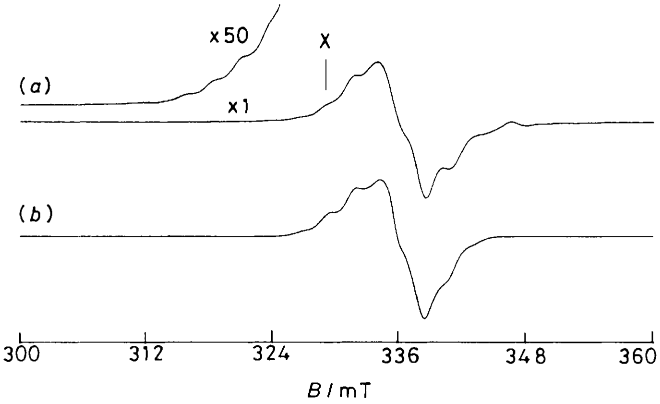

Figure 3. (*a*) Frozen-solution e.p.r. spectrum at 20 K of complex (**2**) with the natural-abundance isotope mixture at microwave frequency 9.436 GHz and power 0.2 mW using 5-mT field modulation at 100 KHz. (*b*) Simulation of (*a*) using the parameters of Table 3

ENDOR Spectroscopy: Determination of Interatomic Distances.—Information on the distance from the paramagnetic molybdenum centre to the methyl hydrogen atoms is contained in the dipolar contribution to the anisotropic hyperfine interaction. In principle this can be determined from single-crystal or frozen-solution e.p.r. spectra. In our case complex (**2**) is not isolable and the anisotropies introduced in the frozen-solution e.p.r. spectrum obscure the details of the ^{1}H interactions. We therefore turned to an analysis by ENDOR techniques because weak hyperfine splittings that are not observable by e.p.r. spectroscopy can be resolved by this double-resonance spectroscopy.

The Mo ··· ^{1}H(*methyl*) *interatomic distance.* Figure 4(*a*) shows ENDOR spectra measured at point X in Figure 3(*a*) for a frozen anolyte solution of complex (**2**) with the natural isotope mixture. Lines A,A′ in Figure 4(*a*), centred on the ^{1}H Zeeman frequency (14.05 MHz), correspond to the methyl ^{1}H nuclei and have a similar value of mean hyperfine coupling (9.8 MHz) to that observed in the room-temperature e.p.r. spectrum (10.1 MHz). These lines disappear for [^{2}H]methyl-labelled (**2**) as shown by Figure 4(*b*). They are replaced by lines B,B′ centred on the free ^{2}H resonance frequency (2.2 MHz) and split by 1.4 MHz, a value related to the 9.8-MHz interaction of ^{1}H by the ratio of the $^{2}H:^{1}H$ magnetic moments.

A single ^{1}H would give a single pair of ENDOR lines, one each side of the ^{1}H Zeeman frequency, if the hyperfine interaction were purely isotropic. Anisotropy would then split each of these lines into up to six components at g values away from the extremes in a low-symmetry environment.[13] Figure 5 shows how the ENDOR spectra of the high-frequency ^{1}H component [A′ in Figure 4(*a*)] vary when measured at different points across the e.p.r. spectrum. At the extremes of the e.p.r. spectrum, the ENDOR spectrum is dominated by single lines, whereas at

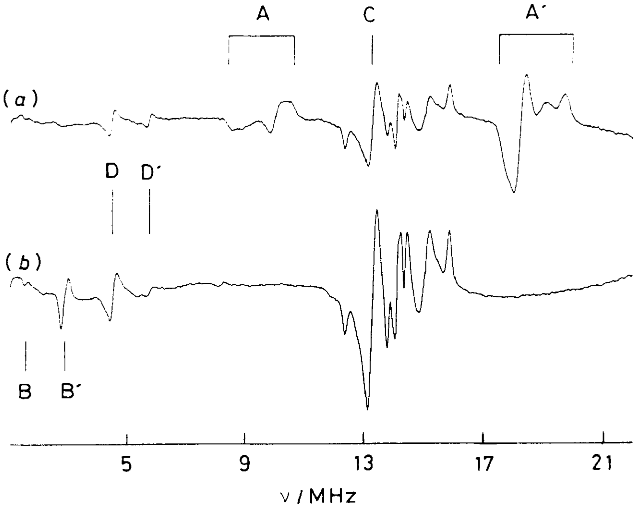

Figure 4. (*a*) ENDOR spectrum at 20 K of complex (**2**) with the natural-abundance isotope mixture measured at point X of Figure 3(*a*). Microwave frequency and power as in Figure 3: the radiofrequency modulation depth was 50 kHz with 1 dB power attenuation. (*b*) ENDOR spectrum of (**2**) with ^{2}H substitution of the methyl protons. Lines A,A′ and B,B′ are assigned to the methyl ^{1}H and ^{2}H nuclei respectively, C to ^{19}F, and D,D′ to ^{14}N (see text)

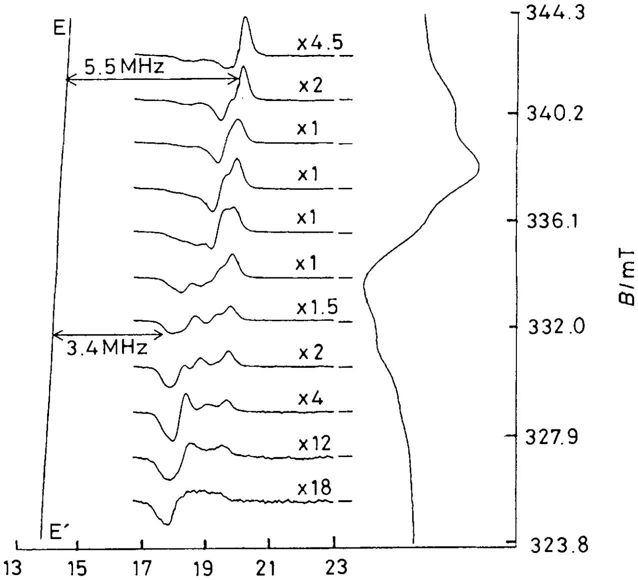

Figure 5. Effect of varying the magnetic field on lines A′ of Figure 4. Measurement conditions as in Figure 4. The spectra were measured at points on the e.p.r. spectrum, shown to the right of the figure, corresponding to the field values marked to the right of the high-frequency baselines of the ENDOR spectra. Relative gains are shown above the spectra. Line E,E′ is the position of the free-proton Zeeman frequency across the e.p.r. spectrum. The arrows show the maximum and minimum values of the separations of the positions of ENDOR features from the free-proton frequency and correspond to one half of the extremes of the hyperfine interaction (see text)

intermediate positions the ENDOR lineshape is more complex and contains several main components.

This is consistent with there being one class of methyl ^{1}H atoms with a large isotropic hyperfine interaction and a smaller anisotropic term. It has been shown that even in a low-symmetry environment the extreme values of an anisotropic hyperfine interaction can be extracted from such a series of ENDOR spectra as that shown in Figure 5 by observing the extremes of movement of the ENDOR lines.[13] From Figure 5 we estimate the extremes to correspond to a minimum of 6.8 and a maximum of 11.0 MHz. Because neither of these extreme lines shifts across the free-proton frequency, they are of the same sign and thus their difference gives a maximum anisotropy of 4.2 MHz.

There are two main contributions to an anisotropic interaction: (*i*) the dipolar electron–nuclear interaction and (*ii*) second-order exchange terms of the order $(\Delta g/g)A_{\text{iso}}$.[14] We estimate from the data given in Tables 2 and 3 that in our case the second-order exchange terms are *ca.* 0.2 MHz, therefore the dipolar terms must dominate. Assuming point dipoles, the dipolar interaction gives splittings with A axial of the form $g_e\beta_e g_n\beta_n(3\cos^2\varphi - 1)/hr^3$ where φ is the azimuthal angle away from $A_{\parallel}$ ($A_{\parallel}$ is along the line joining the centre of electron spin density to the nucleus) and r is the electron–nucleus distance. The maximum anisotropy is $3g_e\beta_e g_n\beta_n/hr^3$ (φ = 0 and 90°) and setting this to 4.2 MHz gives a value of r, the distance from the electron (on the Mo atom) to each methyl ^{1}H atom of 3.8 ± 0.1 Å. This compares with an average value of 3.62 ± 0.02 Å for the parent compound (**1**) as determined by *X*-ray analysis.

The other lines in Figure 4 centred on the ^{1}H Zeeman frequency are presumably from the protons of the ethylene bridge and phenyl rings of the diphosphine ligands; these have not been assigned. A distant ENDOR line at the ^{19}F Zeeman frequency [C in Figure 4(*a*)] can be assigned to fluorine in the $[BF_4]^-$ electrolyte and in the solvent CF_3CO_2H.

The Mo ··· ^{13}C(*methyl*) *interatomic distance.* When complex (**2**) is prepared by electro-oxidation of [^{13}C]methyl-labelled (**1**) the e.p.r. spectrum of the anolyte shows no additional splittings attributable to this $I = \frac{1}{2}$ nucleus. However the ENDOR spectrum of Figure 6(*c*) shows lines (F,F′) centred on the ^{13}C Zeeman frequency of 3.5 MHz with a splitting of 3.6 MHz. In the same way as for Mo ··· H, we calculate a Mo ··· C distance of 3.2 ± 0.1 Å from the variation in the position of the ^{13}C lines across the e.p.r. spectrum. Here we make an additional assumption that there are no anisotropic contributions to the hyperfine interaction from equally occupied p_x, p_y, and p_z orbitals. The calculated distance is essentially identical to that determined for the parent methylimide cation (**1**).

ENDOR lines of the imide nitrogen and the chloride ligand. Figure 6(*a*) shows ENDOR lines measured at point X of Figure 3(*a*), that are separated by 1.3 MHz (*cf.* twice the ^{14}N Zeeman frequency = 2.0 MHz) centred at 5.0 MHz which is, as expected, close to half of the hyperfine interaction assigned to this nucleus in the room-temperature e.p.r. spectrum (9.5 MHz, Table 2). The splitting, number of features, and their relative intensities vary when ENDOR is excited at different points of the e.p.r. spectrum. Quadrupolar terms can be significant for ^{14}N (with $I = 1$) and may explain the different intensities of lines D,D′ in Figure 6(*a*) and the lowered splitting between them. We have not attempted to distinguish between dipolar and quadrupolar terms given the limited data obtainable from the frozen-solution ENDOR spectra, nevertheless the observation of this interaction serves to confirm the retention of the N atom in the product (**2**).

As noted above, ^{35,37}Cl interactions are not observable in the e.p.r. spectra of Figures 2 and 3. However Figure 7 shows ENDOR features measured at point X of Figure 3(*a*) that we assign to the high-frequency lines of the ^{35}Cl and ^{37}Cl interactions. These lines are in the correct proportion for the natural abundance of these isotopes and are in positions consistent with *ca.* 1.0 MHz hyperfine interaction for each. The complementary lines of these pairs would be at too low a frequency to be observable with our spectrometer. Thus ENDOR spectroscopy provides evidence for the retention of the

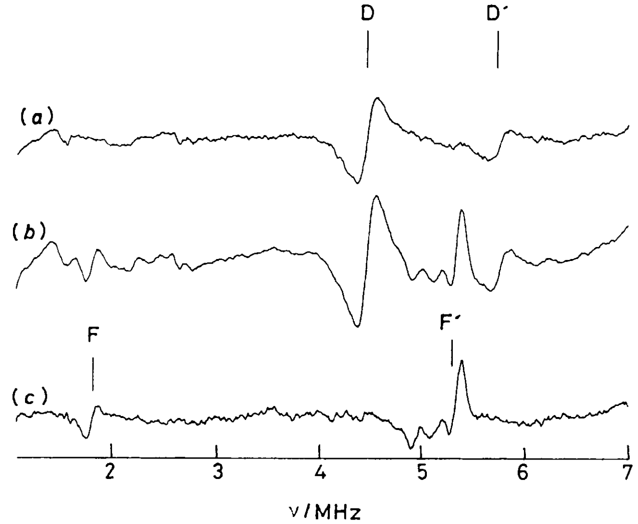

Figure 6. (*a*) ENDOR spectrum of complex (**2**) measured at point X of Figure 3(*a*) under the conditions as in Figure 4. Spectrum (*b*) is of a [^{13}C]methyl-substituted sample and (*c*) is the difference spectrum between (*b*) and (*a*). Lines D,D′ are assigned to ^{14}N and F,F′ to ^{13}C (see text)

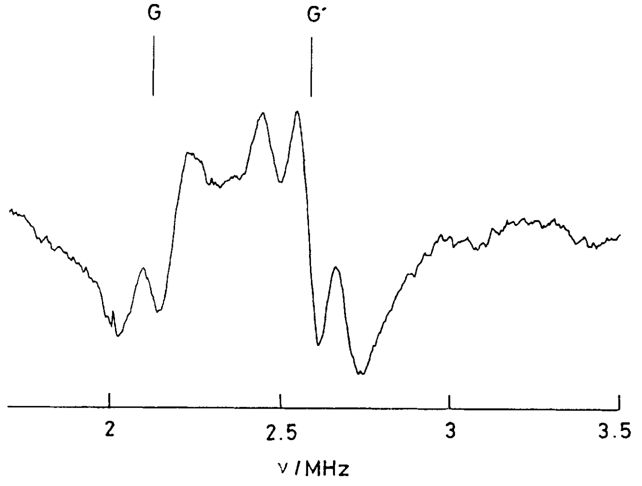

Figure 7. ENDOR spectrum of complex (**2**) showing the lines G,G′ assigned to ^{37}Cl and ^{35}Cl respectively. Conditions as in Figure 4

chloride ligand in complex (**2**), evidence which is unavailable from the e.p.r. data but which is consistent with the reversible electrochemistry.

Conclusion

The comparison of the data determined by *X*-ray crystallography on complex (**1**) with those obtained by e.p.r. and ENDOR measurements on anolyte solutions containing (**2**) leads us to conclude the following.

(*i*) The P, NMe, and Cl ligands of (**1**) are retained in the primary oxidation product (**2**) and are deployed about the paramagnetic molybdenum centre in the configuration of the parent (**1**) which has the P atoms in an essentially square-planar array and the Cl and NMe ligands mutually *trans*.

(*ii*) The single class of ^{1}H-methyl nuclei, the equivalence of the four P atoms, and the Mo ··· H interatomic distance are consistent with the conservation of a linear Mo–N–C arrangement in the product: *sp*^{2} hybridisation to give a nitrogen-centred radical cation and a 16-electron metal centre does not take place.

(*iii*) The Mo ··· ^{13}C interatomic distance determined by ENDOR spectroscopy for complex (**2**) is essentially identical to that of (**1**) measured by *X*-ray crystallography and this suggests that oxidation has little effect on the Mo–N bond order.

(*iv*) There is an apparent difference in the Mo ··· H interatomic distances in (**1**) and (**2**) of about 0.2 Å. This may result from the geometrical restraints applied to the methyl group in the *X*-ray analysis, *viz.* a tetrahedral arrangement of bonds about the C atom and C–H distances of 0.98 Å. The intermolecular C–H distance determined by neutron- and electron-diffraction analyses and spectroscopy is *ca.* 1.09 Å,[15] and some distortion of the N–C–H angles from 109.5° would be expected from the interactions with neighbouring phenyl groups.

(*v*) The estimates given in Table 4 indicate that some 5% of spin density is associated with ligand *s* orbitals. We are unable to determine spin density in the ligand π system but it is probable that the unpaired spin is largely metal based.

We have examined a relatively simple reversible electrochemical system and shown that ENDOR spectroscopy is particularly valuable in obtaining otherwise unavailable structural information from an anolyte which contains an unisolable product in the presence of a large excess of an electrolyte. Undoubtedly ENDOR could be applied with considerable advantage in the *ex situ* analysis of the anolytes or catholytes of more complicated electrochemical systems which involve irreversible chemistry and structural reorganisation.

Experimental

Crystal Structure Analysis of trans-[MoCl(NMe)(Ph_2P-$CH_2CH_2PPh_2)_2$]PF_6·CH_2Cl_2.—*Crystal data.* $C_{53}H_{51}ClF_6$-$MoNP_5$·CH_2Cl_2, M = 1 187.2, orthorhombic, space group $Pn2_1a$ (equivalent to no. 33), a = 22.655(1), b = 20.122(1), c = 11.787(1) Å, U = 5 372.8 Å^3, Z = 4, D_c = 1.467 g cm^{-3}, F(000) = 2 424, μ(Mo-K_α) = 5.9 cm^{-1}, λ(Mo-$K_{\bar{\alpha}}$ = 0.71 069 Å.

Crystals are thick, bright orange-red plates; the faces around the edges of the plate are often re-entrant, but all crystals examined were single. After photographic examination, one crystal (*ca.* 0.19 × 0.20 × 0.24 mm) was mounted on our Enraf-Nonius CAD4 diffractometer (with monochromated radiation) for determination of accurate cell parameters (from the goniometer settings of 25 reflections at θ *ca.* 10.5° each in four settings) and measurement of diffraction intensities (to $\theta_{max.}$ = 25°). During processing, these data were corrected for Lorentz and polarisation effects, absorption (from ψ-scan measurements), and negative intensities (by Bayesian statistics); no deterioration correction was necessary.

Of 4 863 unique reflections entered into the SHELX program system,[16] 4 193 had $I > 2\sigma_I$; the E statistics suggested a non-centrosymmetric lattice. The structure was determined by the heavy-atom method and confirmed the space group as $Pn2_1a$ (equivalent to $Pna2_1$) rather than the centrosymmetric *Pnma*. Refinement by block-diagonal least-squares methods[17] gave convergence at R = 0.050 and R' = 0.050 for 4 835 reflections (with $I > \sigma_I$) weighted $w = (\sigma^2_F + 0.001F^2)^{-1}$. All non-hydrogen atoms were refined anisotropically. Hydrogen atoms in the diphosphine ligands and in the dichloromethane molecule were included in idealised positions and set to ride on their bonded C atoms. Two of the three H-atoms of the methylimide ligand were located in a difference map and the position of the third was estimated; these atoms were initially included in the refinement with geometrical restraints, then all their parameters were set to ride on those of the methyl C atom. The thermal parameters of the third of these H atoms rose to an improbable value and we suggest there is some disorder in this methyl group. Final refined atomic co-ordinates are in Table 5.

Table 5. Final atomic co-ordinates (fractional × 10^4) for $[MoCl(NMe)(Ph_2PCH_2CH_2PPh_2)_2]PF_6{\cdot}CH_2Cl_2$ with e.s.d.s in parentheses

Atom	*x*	*y*	*z*
Mo	1 664.9(2)	2 500	2 620.0(4)
P(1)	1 136.0(7)	3 164.1(9)	4 153(1)
C(11a)	1 650(3)	3 300(4)	5 320(6)
C(12a)	1 738(4)	2 850(6)	6 176(8)
C(13a)	2 183(5)	2 916(7)	6 922(9)
C(14a)	2 550(4)	3 430(7)	6 869(8)
C(15a)	2 472(4)	3 912(7)	6 053(9)
C(16a)	2 025(4)	3 832(5)	5 265(7)
C(11b)	761(3)	3 960(3)	4 043(6)
C(12b)	797(3)	4 341(4)	3 065(7)
C(13b)	494(4)	4 960(4)	3 023(8)
C(14b)	179(3)	5 172(5)	3 951(8)
C(15b)	141(3)	4 788(4)	4 911(8)
C(16b)	435(3)	4 197(4)	4 953(7)
C(1)	532(3)	2 662(3)	4 726(6)
C(2)	654(3)	1 922(4)	4 635(6)
P(2)	876.6(7)	1 677.3(9)	3 208(2)
C(21a)	194(3)	1 642(3)	2 380(6)
C(22a)	251(3)	1 569(4)	1 218(7)
C(23a)	−241(4)	1 547(5)	533(8)
C(24a)	−799(3)	1 599(5)	1 005(9)
C(25a)	−848(3)	1 675(6)	2 172(9)
C(26a)	−352(3)	1 698(4)	2 864(8)
C(21b)	1 085(3)	800(3)	3 405(6)
C(22b)	950(4)	324(4)	2 621(7)
C(23b)	1 107(4)	−321(4)	2 769(8)
C(24b)	1 414(4)	−510(4)	3 732(8)
C(25b)	1 573(4)	−29(4)	4 513(8)
C(26b)	1 406(3)	617(4)	4 375(7)
P(3)	2 340.6(7)	3 385.6(9)	1 762(2)
C(31a)	3 098(3)	3 394(4)	2 299(6)
C(32a)	3 198(3)	3 321(4)	3 428(7)
C(33a)	3 774(4)	3 371(5)	3 863(9)
C(34a)	4 238(3)	3 499(5)	3 150(10)
C(35a)	4 136(4)	3 546(6)	2 009(10)
C(36a)	3 574(3)	3 502(4)	1 576(8)
C(31b)	2 180(3)	4 272(3)	1 662(6)
C(32b)	2 414(4)	4 723(4)	2 401(7)
C(33b)	2 284(5)	5 397(5)	2 346(9)
C(34b)	1 900(4)	5 617(5)	1 502(8)
C(35b)	1 655(4)	5 182(5)	771(8)
C(36b)	1 789(3)	4 519(4)	823(7)
C(3)	2 397(3)	3 162(4)	263(6)
C(4)	2 595(3)	2 446(4)	136(5)
P(4)	2 121.3(7)	1 861.0(9)	970(1)
C(41a)	1 662(3)	1 461(4)	−112(6)
C(42a)	1 599(3)	776(4)	−115(8)
C(43a)	1 236(4)	468(5)	−902(9)
C(44a)	936(4)	845(7)	−1 700(10)
C(45a)	991(4)	1 545(7)	−1 707(8)
C(46a)	1 360(3)	1 833(5)	−902(6)
C(41b)	2 645(3)	1 205(3)	1 312(6)
C(42b)	2 587(3)	834(4)	2 276(6)
C(43b)	2 986(4)	329(5)	2 528(8)
C(44b)	3 451(4)	208(6)	1 795(10)
C(45b)	3 502(4)	549(5)	831(9)
C(46b)	3 103(3)	1 067(4)	552(7)
Cl(5)	956.8(7)	2 983.2(9)	1 228(2)
N(6)	2 156(2)	2 178(3)	3 604(4)
C(61)	2 580(3)	1 923(5)	4 388(7)
P(7)	−872(1)	2 333(1)	7 022(2)
F(71)	−977(4)	2 687(8)	8 154(7)
F(72)	−269(4)	2 605(9)	7 030(9)
F(73)	−1 484(4)	2 022(7)	6 985(8)
F(74)	−768(4)	2 042(7)	5 871(8)
F(75)	−680(8)	1 787(9)	7 697(14)
F(76)	−1 144(8)	2 890(6)	6 435(12)
C(9)	245(5)	3 688(6)	−1 091(10)
Cl(91)	879(1)	3 618(2)	−1 837(3)
Cl(92)	122(2)	4 494(2)	−556(4)

In a final difference map all the highest peaks (to 0.65 e Å^{-3}) are in the region of the $[PF_6]^-$ ion where some of the thermal parameters are also quite high; there is either considerable motion or some site disorder in this anion.

Scattering factors for neutral atoms were from ref. 18. Computer programs have been noted in refs. 16 and 17, and in Table 4 of ref. 19; they were run on the MicroVAX II machine in this Laboratory.

Additional material available from the Cambridge Crystallographic Data Centre comprises H-atom co-ordinates, thermal parameters, and remaining bond distances and angles.

Electrolyses.—The complex *trans*-$[MoCl(NMe)(Ph_2PCH_2CH_2PPh_2)_2]I$ was synthesised by the literature method.[20] Because the counter ion I^- is electroactive at potentials near that of the methylimido-cation it was exchanged for $[PF_6]^-$ by metathesis with $Tl[PF_6]$ (**CAUTION**: poisonous). Carbon-13- and ^2H-labelled methyl iodide were used to prepare the isotopically labelled complexes.

Controlled-potential electrolyses were carried out in a four-compartment, three-electrode H-type cell in which the working electrode was a platinum gauze of nominal area 2 cm^2. General procedures for the preparative electrolyses, coulometry, and voltammetric measurements together with a description of instrumentation have been provided elsewhere.[21] Samples of anolyte containing complex (**2**) were transferred from the cell to e.p.r. tubes by gas-tight syringe.

All manipulations of the complexes and electrolytes were carried out under an atmosphere of dinitrogen.

E.P.R. and ENDOR Measurements.—E.p.r. and ENDOR spectra were measured on an updated Bruker ER200D-SRC spectrometer fitted with an ENDOR/TRIPLE accessory with a radiofrequency amplifier of 100 W nominal output power. Samples were cooled using an Oxford Instruments ESR 900 cryostat.

Acknowledgements

We thank Drs. R. C. Bray and B. D. Howes for helpful discussion. The work was supported by a Link Research Grant from the A.F.R.C.

References

1 D. L. Hughes, M. Y. Mohammed, and C. J. Pickett, *J. Chem. Soc., Chem. Commun.*, 1989, 1399.

2 M. Y. Mohammed and C. J. Pickett, *J. Chem. Soc., Chem. Commun.*, 1988, 1119.

3 J-G. Li, B. K. Burgess, and J. L. Corbin, *Biochemistry*, 1982, **21**, 4393.

4 D. J. Lowe, K. Fisher, R. N. F. Thorneley, S. Vaughn, and B. K. Burgess, *Biochemistry*, 1989, **28**, 8460.

5 D. L. Hughes, D. J. Lowe, M. Y. Mohammed, C. J. Macdonald, and C. J. Pickett, *Polyhedron*, 1989, **8**, 1653.

6 A. M. Bond and K. B. Oldham, *J. Phys. Chem.*, 1983, **87**, 2492.

7 J. R. Dilworth, P. L. Dahlstrom, J. R. Hyde, and J. Zubieta, *Inorg. Chim. Acta*, 1983, **71**, 21.

8 D. C. Bradley, M. B. Hursthouse, K. M. A. Malik, A. J. Nielson, and R. L. Short, *J. Chem. Soc., Dalton Trans.*, 1983, 2651.

9 O. Hammerich, N. S. Moe, and V. D. Parker, *J. Chem. Soc., Chem. Commun.*, 1972, 156.

10 C. J. Pickett and D. Pletcher, *J. Chem. Soc., Dalton Trans.*, 1976, 636.
11 J. H. Enemark and W. E. Cleland, jun., *Polyhedron*, 1986, **5**, 423.
12 J. Morton and K. F. Preston, *J. Magn. Reson.*, 1978, **30**, 577.
13 B. M. Hoffman, R. A. Venters, and J. Martinsen, *J. Magn. Reson.*, 1985, **62**, 537.
14 T. Moriya, in 'Magnetism,' eds. G. T. Rado and H. Suhl, Academic Press, New York and London, 1963, vol. 1, pp. 85–125.
15 See, *e.g.*, L. Pauling, 'The Nature of the Chemical Bond,' 3rd edn., Cornell University Press, Ithaca, New York, 1960, p. 226.
16 G. M. Sheldrick, SHELX 76, Program for crystal structure determination, University of Cambridge, 1976.
17 J. D. Owen, BLOKLS, Program for block-diagonal least-squares refinement, Rothamsted Experimental Station, Harpenden, 1981.
18 'International Tables for *X*-Ray Crystallography,' Kynoch Press, Birmingham, 1974, vol. 4, pp. 99 and 149.
19 S. N. Anderson, R. L. Richards, and D. L. Hughes, *J. Chem. Soc., Dalton Trans.*, 1986, 245.
20 J. Chatt and J. R. Dilworth, *J. Chem. Soc., Chem. Commun.*, 1975, 983.
21 T. I. Al Salih and C. J. Pickett, *J. Chem. Soc., Dalton Trans.*, 1985, 1255.

Received 10*th November* 1989; *Paper* 9/04837E